Towards multi-body multi-rotors for long reach manipulation

Connor J. Boss*, Vishal Abhishek*, and Vaibhav Srivastava

***Abstract*— We design a novel multi-body Unmanned Aerial Vehicle (UAV) to be used for long reach manipulation tasks. We consider the modeling and control of a multi-body multi-rotor system in which a horizontally actuated bi-rotor platform is suspended from a larger multi-rotor through a passive revolute joint. We provide dynamic modeling, feedback linearizing control through the use of flat outputs, and an extended high-gain observer (EHGO) based output feedback control design assuming that the system operates in a plane. Simulation results are provided to show the long reach manipulator platform tracking a trajectory. The methods are rigorously analyzed and stability of the closed-loop system under output feedback is proven.**

I. INTRODUCTION

Unmanned Aerial Vehicles (UAVs) have been developed to perform a variety of tasks including remote infrastructure inspection, surveillance, tool operation, and package delivery. As many fields become increasingly reliant on UAVs, advanced systems are required which can actively interact with the environment and perform challenging tasks in unstructured environments.

Augmenting a UAV with another multi-body system, e.g., a manipulator, significantly increases its functionality. Several UAV-manipulator systems, often referred to as aerial manipulators, have been designed for aerial pick and place [1], avian inspired grasping and perching [2, 3], mobile manipulation [4–6], assembly [7], valve turning [8], and aerial phytobiopsy [9]. Having a manipulator connected to a UAV through an actuated joint is a typical design for such systems. However, this limits the range of operation of the end-effector with respect to the UAV.

In recent years a variety of alternate designs, in which a UAV connected to another system through a passive joint, have been considered. Using cables to suspend a load from a UAV is one such example. Transporting a load using suspended cables has been considered both in single-UAV [10–12] as well as multi-UAV scenarios [13–16]. Several researchers have also considered using a passive spherical joint to attach a rigid link to the UAV. For example, the authors in [17] consider a rigid rod suspended at one end from a UAV through a spherical joint and study scenarios with both a torque-actuated and an actuation-free joint. In [18] a spherically connected multiquadrotor (SmQ) platform is designed in which multiple quadrotors are used as rotating thrust generators for the platform.

Aerial manipulators specifically designed for long reach manipulation have recently gained attention. In [19], a dual arm connected at the end of a flexible link attached to a UAV is designed. In [20] and [21], a manipulator arm is connected at the end of a rod and a platform, respectively, which in turn are attached to the UAV through a passive spherical joint and act as a pendulum. In [22, 23], two methods of designing a suspended platform from a larger aerial carrier using cables are presented. The platforms are actuated through winches and rotors and have manipulators mounted on the platforms to be used for manipulation tasks. Another approach [24] shows a dual arm manipulator suspended below a carrier UAV for long reach manipulation and inspection tasks. In these approaches, the manipulator is suspended directly below the carrier UAV, whereas our approach allows the manipulator platform to swing out from under the carrier UAV to reach areas unaffected by downdraft.

Large UAVs may be required in situations where heavy lift capabilities are needed. However, several applications require access to locations where a large UAV is not well suited to operate in close proximity to the manipulated object. This can be due to factors such as heavy downdraft generated by the UAV, confined work spaces, or higher required operational accuracy. One such example is remote crop sampling, in which the downdraft from the UAV disturbs the crops and makes sampling difficult. Cleaning high-rise windows or solar panels is another example where it can be difficult to get close enough with a large UAV, but heavy lift capabilities are necessary to carry the cleaning products.

In this paper, we address these challenges by presenting a novel aerial manipulator. The proposed system consists of a bi-rotor actuated platform connected to a rigid rod which is suspended from a carrier UAV through a passive revolute joint. The presence of the passive revolute joint and the actuation of the platform using rotor thrust form the novel aspects of our design. The proposed aerial manipulator can be used for the long reach manipulation tasks presented above in which a larger UAV is required, however may not be well suited. Consider the case of remote crop sampling. Our design would allow the small suspended manipulator platform to swing out to the side below the large carrier UAV to escape the downdraft. The horizontal bi-rotor actuation of the platform has the added benefit that it only produces air currents perpendicular to the manipulator, leaving the work space free from induced disturbances.

We analyze and control the system assuming its operations are restricted to a plane. The system dynamics are formulated using the Lagrangian approach and it is shown that the bi-

* Equal contribution.

This work has been supported in part by a NASA Michigan Space Grant Consortium Fellowship under award number NNX15AJ20H and ARO grant W911NF-18-1-0325.

Connor J. Boss and Vaibhav Srivastava are with the Electrical and Computer Engineering, Michigan State University, East Lansing, MI 48824-1226, USA vaibhav at egr.msu.edu

Vishal Abhishek is with the Department of Mechanical Engineering, Michigan State University, East Lansing, MI 48824-1226, USA abhishe3 at egr.msu.edu

rotor platform pose, i.e., position and orientation, act as differentially flat outputs. An extended high-gain observer (EHGO) is designed to estimate states and disturbances acting on the system, which is an extension of our earlier work [25, 26]. An output feedback linearizing control law is designed for flat output trajectory tracking considering the coupled UAV-platform dynamics. The result is a feedback linearizing control approach that is robust to modeling error and disturbances. Simulation results are provided to illustrate the effectiveness of the methods employed where external disturbances are applied, estimated, and canceled through the feedback linearizing control design. The system is rigorously analyzed to prove stability.

The remainder of the paper is organized in the following manner. Section II gives the design and modeling of the aerial manipulator whereas Section III details the control design using the EHGO. Section IV proves stability of the system, and Section V provides simulation results. Finally, Section VI concludes the paper.

II. System Modeling

We study a rigid platform with bi-rotor actuation, rigidly attached to a rigid rod connected at the other end to a carrier UAV through a passive revolute joint. The suspended platform is actuated with two rotors so as to provide a net thrust perpendicular to the rod with no net moment. The two rotors attached at both ends of the platform are operated with angular velocity in opposite directions to generate viscous torque in opposite directions while generating thrust in the same direction. Thus, when operated at the same speed, the rotors generate a net thrust along the axis of the platform with no net moment. The resulting multi-body system is shown in Fig. 1. For the analysis going forward, we restrict our case to planar motion in the vertical plane.

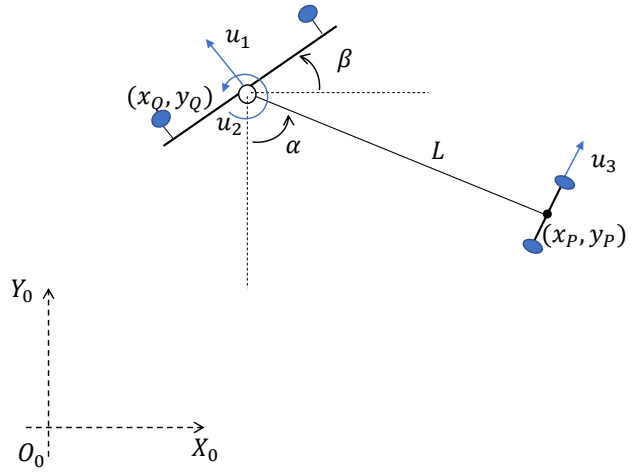

Fig. 1. Carrier UAV with suspended bi-rotor actuated platform.

A. Dynamic Model

We introduce the following notation. Unless otherwise stated, all coordinates are expressed in the inertial frame:

m_Q	mass of the carrier UAV
m_P	mass of the platform
L	length of the rod
(x_Q, y_Q)	position coordinates of the carrier UAV center of mass
(x_P, y_P)	position coordinates of the platform center of mass
α	angular position of the platform
β	angular position of the carrier UAV
I_Q	Moment of Inertia of the carrier UAV in the body-frame
I_P	Moment of Inertia of the platform in the body-frame
u_1	total rotor thrust on the carrier UAV
u_2	torque on the carrier UAV about its center of mass
u_3	total platform thrust
g	acceleration due to gravity

We assume the revolute joint and the connecting rod are rigidly attached to the platform and are massless. The centers of mass of the carrier UAV and the platform are assumed to be at their geometric centers and are the same as the two end-points of the connecting rod. The actuator forces are the total carrier UAV thrust, u_1, the carrier UAV moment, u_2, and the suspended platform thrust, u_3. These forces are shown in Fig. 1.

The equations of motion are written using x_P, y_P, α, and β as generalized coordinates. The kinetic energy, T, and the potential energy, U, are given by

$$\begin{aligned} T &= \frac{1}{2}(m_P + m_Q)(\dot{x}_P^2 + \dot{y}_P^2) - m_Q L(\dot{x}_P \dot{\alpha} c_\alpha + \dot{y}_P \dot{\alpha} s_\alpha) \\ &\quad + \frac{1}{2} I_Q \dot{\beta}^2 + \frac{1}{2}(I_P + m_Q L^2)\dot{\alpha}^2, \\ U &= m_Q g(y_P + L c_\alpha) + m_P g y_P. \end{aligned}$$

The corresponding generalized forces are

$$\begin{aligned} \mathcal{F}_{x_P} &= u_3 c_\alpha - u_1 s_\beta, \\ \mathcal{F}_{y_P} &= u_3 s_\alpha + u_1 c_\beta, \\ \mathcal{F}_\alpha &= u_1 L s_{(\beta-\alpha)}, \\ \mathcal{F}_\beta &= u_2. \end{aligned}$$

Here, c_α and s_α represent $\cos\alpha$ and $\sin\alpha$ respectively. The equations of motion can be written compactly as

$$M(\boldsymbol{q}_1)\ddot{\boldsymbol{q}}_1 + C(\boldsymbol{q}_1, \dot{\boldsymbol{q}}_1)\dot{\boldsymbol{q}}_1 + G(\boldsymbol{q}_1) = \boldsymbol{\tau}, \tag{1a}$$

$$I_Q \ddot{\beta} = u_2, \tag{1b}$$

where, $\boldsymbol{q}_1 := [x_P, y_P, \alpha]^\top$, $\boldsymbol{\tau} := [\mathcal{F}_{x_P}, \mathcal{F}_{y_P}, \mathcal{F}_\alpha]^\top$, and

$$\begin{aligned} M &= \begin{bmatrix} (m_P + m_Q) & 0 & -m_Q L c_\alpha \\ 0 & (m_P + m_Q) & -m_Q L s_\alpha \\ -m_Q L c_\alpha & -m_Q L s_\alpha & (I_P + m_Q L^2) \end{bmatrix}, \\ C &= \begin{bmatrix} 0 & 0 & m_Q L \dot{\alpha} s_\alpha \\ 0 & 0 & -m_Q L \dot{\alpha} c_\alpha \\ 0 & 0 & 0 \end{bmatrix}, \\ G &= \begin{bmatrix} 0 & (m_P + m_Q) g & -m_Q g L s_\alpha \end{bmatrix}^\top. \end{aligned} \tag{2}$$

B. Differential flatness

The system has four generalized coordinates at the position level: x_P, y_P, α, and β, but only three independent control inputs: u_1, u_2, and u_3, thus resulting in one degree of underactuation. It can be seen from (1a) and the expression for $\boldsymbol{\tau}$ that designing a trajectory in $\boldsymbol{q}_1$ uniquely determines the trajectories of u_1, u_3, and β. Furthermore, a trajectory in β uniquely determines u_2. Thus, a trajectory in $\boldsymbol{q}_1$ uniquely determines all state trajectories and control inputs. As a result, $\boldsymbol{q}_1$ are the differentially flat outputs.

C. State-Space Model

The dynamics can now be written as two subsystems in state-space form. Defining $\boldsymbol{q}_2 := \dot{\boldsymbol{q}}_1$, $\boldsymbol{q} := [\boldsymbol{q}_1^\top, \boldsymbol{q}_2^\top]^\top$, the platform dynamics become

$$\begin{aligned} &\dot{\boldsymbol{q}}_1 = \boldsymbol{q}_2, \\ &\dot{\boldsymbol{q}}_2 = M(\boldsymbol{q}_1)^{-1}[-C(\boldsymbol{q})\boldsymbol{q}_2 - G(\boldsymbol{q}_1)] + M(\boldsymbol{q}_1)^{-1}\boldsymbol{\tau} + \boldsymbol{\sigma}_q, \end{aligned} \tag{3}$$

where $\boldsymbol{\sigma}_q \in \mathbb{R}^3$ is an added term to represent the lumped disturbance in the platform subsystem, which satisfies the following assumption.

Assumption 1 (Properties of Disturbances): For a control system with state $\boldsymbol{x} \in \mathbb{R}^n$, expressed in lower triangular form, such as (3), any disturbance term is assumed to enter only the $\boldsymbol{x}_n$ dynamics. The disturbance term is also assumed to be continuously differentiable and its partial derivatives with respect to states are bounded on compact sets of those states for all $t \geq 0$.

Defining $\beta_1 := \beta$, $\beta_2 := \dot{\beta}$, and $\boldsymbol{\beta} = [\beta_1, \beta_2]^\top$ the carrier UAV orientation dynamics become

$$\begin{aligned} \dot{\beta}_1 &= \beta_2, \\ \dot{\beta}_2 &= \frac{u_2}{I_Q} + \sigma_\beta, \end{aligned} \tag{4}$$

where $\sigma_\beta \in \mathbb{R}$ is an added term to represent the lumped disturbance in the carrier UAV subsystem, which also satisfies *Assumption 1*.

Let $\boldsymbol{q}^d(t) = [x_P^d, y_P^d, \alpha^d]^\top$ be the desired output trajectory and let $\beta^c(t)$ be the desired orientation of the carrier UAV. By making the following change of variables

$$\begin{aligned} &\boldsymbol{e}_1 = \boldsymbol{q}_1 - \boldsymbol{q}^d, \quad \boldsymbol{e}_2 = \dot{\boldsymbol{e}}_1 = \boldsymbol{q}_2 - \dot{\boldsymbol{q}}^d, \quad \boldsymbol{e} = [\boldsymbol{e}_1^\top,\ \boldsymbol{e}_2^\top]^\top, \\ &\tilde{\beta}_1 = \beta_1 - \beta^c, \quad \tilde{\beta}_2 = \dot{\tilde{\beta}}_1 = \beta_2 - \dot{\beta}^c, \quad \tilde{\boldsymbol{\beta}} = [\tilde{\beta}_1,\ \tilde{\beta}_2]^\top, \end{aligned}$$

the system can be written in terms of tracking error as

$$\begin{aligned} \dot{\boldsymbol{e}}_1 &= \boldsymbol{e}_2, \\ \dot{\boldsymbol{e}}_2 &= f(\boldsymbol{q}_1, \boldsymbol{e}, \dot{\boldsymbol{q}}^d) + M(\boldsymbol{q}_1)^{-1}\boldsymbol{\tau} + \boldsymbol{\sigma}_q - \ddot{\boldsymbol{q}}^d, \\ \dot{\tilde{\beta}}_1 &= \tilde{\beta}_2, \\ \dot{\tilde{\beta}}_2 &= \frac{u_2}{I_Q} + \varsigma_\beta, \end{aligned} \tag{5}$$

where $f(\boldsymbol{q}_1, \boldsymbol{e}, \dot{\boldsymbol{q}}^d) = M(\boldsymbol{q}_1)^{-1}[-C(\boldsymbol{q}_1, \boldsymbol{e}_2 + \dot{\boldsymbol{q}}^d)(\boldsymbol{e}_2 + \dot{\boldsymbol{q}}^d) - G(\boldsymbol{q}_1)]$ and $\ddot{\beta}^c$ is lumped into the disturbance term $\varsigma_\beta = \sigma_\beta - \ddot{\beta}^c$. The advantage of this modification is we no longer require higher-order derivatives of β^c, however β^c must be third order differentiable to ensure ς_β satisfies *Assumption 1*.

III. Control Design

We begin by designing a state feedback control law for each subsystem using feedback linearization, thus requiring the assumption that all states and disturbances are known. This assumption will then be relaxed by introducing an EHGO to estimate all states and disturbances to arrive at an output feedback control law.

A. State Feedback Control

Using the differentially flat outputs, $\boldsymbol{q}_1$, we design a trajectory tracking controller by taking the control input $\boldsymbol{\tau}^c := M(\boldsymbol{q}_1)[-k_1\boldsymbol{e}_1 - k_2\boldsymbol{e}_2 - \boldsymbol{\sigma}_q + \ddot{\boldsymbol{q}}^d - f(\boldsymbol{q}_1, \boldsymbol{e}, \dot{\boldsymbol{q}}^d)]$. Take β^c as the desired orientation of the carrier UAV, and use the expression for $\boldsymbol{\tau}$ at $\beta = \beta^c$ to compute u_3^c, u_1^c, and β^c from the equation $\boldsymbol{\tau}_{(\beta=\beta^c)} = \boldsymbol{\tau}^c = [\tau_1^c, \tau_2^c, \tau_3^c]^\top$. This leads to the following feedback linearizing control equations

$$\begin{aligned} u_3^c &= \tau_1^c c_\alpha + \tau_2^c s_\alpha + \tau_3^c / L, \\ u_1^c &= \sqrt{(u_3^c c_\alpha - \tau_1^c)^2 + (\tau_2^c - u_3^c s_\alpha)^2}, \\ \beta^c &= \operatorname{atan2}((u_3^c c_\alpha - \tau_1^c), (\tau_2^c - u_3^c s_\alpha)). \end{aligned} \tag{6}$$

Note that for β^c to be third order differentiable, we require the desired trajectory, $\boldsymbol{q}^d$, to be fifth order differentiable. If we set the control actions $u_1 = u_1^c, u_3 = u_3^c$, and $u_2 = I_Q(-k_3\tilde{\beta}_1 - k_4\tilde{\beta}_2 - \varsigma_\beta)$ the closed-loop system dynamics become

$$\dot{\boldsymbol{e}} = A_{\boldsymbol{e}}\boldsymbol{e} + \begin{bmatrix} 0_{3\times 1} \\ \boldsymbol{e}_\beta(t, \boldsymbol{q}_1, \tilde{\beta}_1) \end{bmatrix}, \tag{7a}$$

$$\dot{\tilde{\boldsymbol{\beta}}} = A_{\tilde{\boldsymbol{\beta}}}\tilde{\boldsymbol{\beta}}, \tag{7b}$$

where

$$A_{\boldsymbol{e}} = \begin{bmatrix} 0_3 & I_3 \\ -k_1 I_3 & -k_2 I_3 \end{bmatrix}, \quad A_{\tilde{\boldsymbol{\beta}}} = \begin{bmatrix} 0 & 1 \\ -k_3 & -k_4 \end{bmatrix},$$

$$\boldsymbol{e}_\beta(t, \boldsymbol{q}_1, \tilde{\beta}_1) = M^{-1}(\boldsymbol{q}_1) \begin{bmatrix} u_1^c(s_\beta - s_{\beta^c}) \\ u_1^c(c_{\beta^c} - c_\beta) \\ u_1^c L(s_{(\beta^c - \alpha)} - s_{(\beta - \alpha)}) \end{bmatrix},$$

and $I_3 \in \mathbb{R}^{3\times 3}$ is the identity matrix, $0_3 \in \mathbb{R}^{3\times 3}$ is a matrix of zeros, and $0_{3\times 1} \in \mathbb{R}^3$ is a vector of zeros. As a result, the two closed-loop subsystems form a cascade connection through $\boldsymbol{e}_\beta$ and the fact that $\boldsymbol{e}_\beta(t, \boldsymbol{q}_1, 0) = 0$ is important when analyzing stability of the cascaded system. Note that $\tilde{\beta}_2$ and ς_β contain $\dot{\beta}^c$ and $\ddot{\beta}^c$ respectively. We do not compute these derivatives directly, however the terms containing them are estimated completely by the EHGO in the output feedback control design.

B. Extended High-Gain Observer Design

We now present the design of an EHGO to estimate unmeasured states as well as uncertainties in the form of modeling error and external disturbances. These estimates will be used to cancel out the uncertainties in the control design, resulting in improved performance of the feedback linearizing controllers. For the EHGO design we assume only the position level states can be measured. We begin

by extending the tracking error dynamics (5) to include disturbance dynamics

$$\begin{aligned}
\dot{\boldsymbol{e}}_1 &= \boldsymbol{e}_2,\\
\dot{\boldsymbol{e}}_2 &= f(\boldsymbol{q}_1, \boldsymbol{e}, \dot{\boldsymbol{q}}^d) + M(\boldsymbol{q}_1)^{-1}\boldsymbol{\tau} + \boldsymbol{\sigma}_q - \ddot{\boldsymbol{q}}^d,\\
\dot{\boldsymbol{\sigma}}_q &= \varphi_q(t, \boldsymbol{e}),\\
\dot{\tilde{\beta}}_1 &= \tilde{\beta}_2,\\
\dot{\tilde{\beta}}_2 &= \frac{u_2}{I_Q} + \varsigma_\beta,\\
\dot{\sigma}_\beta &= \varphi_\beta(t, \tilde{\boldsymbol{\beta}}),
\end{aligned} \tag{8}$$

where $\varphi_q(t, \boldsymbol{e})$ and $\varphi_\beta(t, \tilde{\boldsymbol{\beta}})$ are unknown functions describing the disturbance dynamics and are assumed to be continuous and bounded on any compact set in $\boldsymbol{e}$ and $\tilde{\boldsymbol{\beta}}$ to ensure *Assumption 1* is satisfied.

To facilitate writing the observer dynamics in a compact form, we define the state vector $\boldsymbol{\chi} = [\boldsymbol{e}_1^\top, \boldsymbol{e}_2^\top, \boldsymbol{\sigma}_q^\top, \tilde{\beta}_1, \tilde{\beta}_2, \sigma_\beta]^\top$, and the disturbance function vector $\varphi(t, \boldsymbol{e}, \tilde{\boldsymbol{\beta}}) = [\varphi_q(t, \boldsymbol{e})^\top, \varphi_\beta(t, \tilde{\boldsymbol{\beta}})]^\top$, leading to the observer dynamics

$$\begin{aligned}
\dot{\hat{\boldsymbol{\chi}}} &= A\hat{\boldsymbol{\chi}} + B\left[\bar{f}(\boldsymbol{q}_1, \hat{\boldsymbol{e}}, \dot{\boldsymbol{q}}^d) + \bar{G}(\boldsymbol{q}_1)\boldsymbol{u}\right] + H\hat{\boldsymbol{\chi}}_e,\\
\hat{\boldsymbol{\chi}}_e &= C(\boldsymbol{\chi} - \hat{\boldsymbol{\chi}}),
\end{aligned} \tag{9}$$

where

$$A = \oplus_{i=1}^2 A_i,\ B = \oplus_{i=1}^2 B_i,\ C = \oplus_{i=1}^2 C_i,\ H = \oplus_{i=1}^2 H_i,$$

$$A_1 = \begin{bmatrix} 0_3 & I_3 & 0_3 \\ 0_3 & 0_3 & I_3 \\ 0_3 & 0_3 & 0_3 \end{bmatrix},\ B_1 = \begin{bmatrix} 0_3 \\ I_3 \\ 0_3 \end{bmatrix},\ H_1 = \begin{bmatrix} \rho_1/\epsilon I_3 \\ \rho_2/\epsilon^2 I_3 \\ \rho_3/\epsilon^3 I_3 \end{bmatrix},$$
$$C_1 = \begin{bmatrix} I_3 & 0_3 & 0_3 \end{bmatrix},$$

$$A_2 = \begin{bmatrix} 0 & 1 & 0 \\ 0 & 0 & 1 \\ 0 & 0 & 0 \end{bmatrix},\ B_2 = \begin{bmatrix} 0 \\ 1 \\ 0 \end{bmatrix},\ H_2 = \begin{bmatrix} \rho_1/\epsilon \\ \rho_2/\epsilon^2 \\ \rho_3/\epsilon^3 \end{bmatrix},$$
$$C_2 = \begin{bmatrix} 1 & 0 & 0 \end{bmatrix},$$

$$\bar{f}(\boldsymbol{q}_1, \hat{\boldsymbol{e}}, \dot{\boldsymbol{q}}^d) = \begin{bmatrix} f(\boldsymbol{q}_1, \hat{\boldsymbol{e}}, \dot{\boldsymbol{q}}^d) \\ 0 \end{bmatrix},\quad \bar{G}(\boldsymbol{q}_1) = \begin{bmatrix} M(\boldsymbol{q}_1)^{-1} & 0_{3\times 1} \\ 0_{1\times 3} & 1/I_Q \end{bmatrix},$$
$$\boldsymbol{u} = \begin{bmatrix} \boldsymbol{\tau}^c \\ u_2 \end{bmatrix},$$

where $\oplus$ denotes the matrix direct sum, H is designed by choosing ρ such that

$$s^3 + \rho_1 s^2 + \rho_2 s + \rho_3 = 0,$$

is Hurwitz and $\epsilon \in \mathbb{R}_{>0}$ is a sufficiently small tuning parameter.

C. Output Feedback Control

We now define an output feedback controller to ensure tracking of the desired trajectory, $\boldsymbol{q}^d$. The output feedback controller is designed by replacing the states and disturbances in the state feedback controller by their estimates from the EHGO

$$\hat{\boldsymbol{\tau}}^c := M(\boldsymbol{q}_1)[-k_1\hat{\boldsymbol{e}}_1 - k_2\hat{\boldsymbol{e}}_2 - \hat{\boldsymbol{\sigma}}_q + \ddot{\boldsymbol{q}}^d - f(\boldsymbol{q}_1, \hat{\boldsymbol{e}}, \dot{\boldsymbol{q}}^d)].$$

This leads to the following output feedback control equations

$$\hat{u}_3^c = \hat{\tau}_1^c c_\alpha + \hat{\tau}_2^c s_\alpha + \hat{\tau}_3^c/L, \tag{10a}$$
$$\hat{u}_1^c = \sqrt{(\hat{u}_3^c c_\alpha - \hat{\tau}_1^c)^2 + (\hat{u}_3^c s_\alpha - \hat{\tau}_2^c)^2}, \tag{10b}$$
$$\hat{\beta}^c = \operatorname{atan2}((\hat{u}_3^c c_\alpha - \hat{\tau}_1^c), (\hat{\tau}_2^c - \hat{u}_3^c s_\alpha)), \tag{10c}$$
$$\hat{u}_2 = I_Q(-k_3\hat{\tilde{\beta}}_1 - k_4\hat{\tilde{\beta}}_2 - \hat{\varsigma}_\beta). \tag{10d}$$

The state and disturbance estimates must be saturated outside a compact set of interest to overcome the peaking phenomenon present in EHGOs, see *Remark 1* in [26].

IV. Stability Analysis

The stability of the state feedback control, observer estimates, and output feedback controller will now be proven. We begin by restricting the domain of operation by establishing a compact positively invariant set in which the system will operate. We then prove stability of the closed-loop system under state feedback, convergence of the observer estimates, and finally prove stability of the closed-loop system under output feedback.

A. Restricting Domain of Operation

To ensure the angular position of the carrier UAV, β_1, satisfies $-\pi/2 < \beta_1 < \pi/2$, we restrict the domain of operation and make the following assumption.

Assumption 2: The rotational reference signal β^c remains in the set $\{|\beta^c| < \pi/2 - \delta\}$, where $0 < \delta < \pi/2$.

It can now be shown that for sufficiently small initial tracking error, $\tilde{\boldsymbol{\beta}}(0)$, the tracking error $|\tilde{\beta}_1(t)| < \delta$ for all $t > 0$. Together with *Assumption 2*, this ensures that $|\beta_1| < \pi/2$.

A Lyapunov function in the rotational error dynamics is taken as

$$V_{\tilde{\beta}} = \tilde{\boldsymbol{\beta}}^\top P_{\tilde{\beta}}\tilde{\boldsymbol{\beta}}, \quad \text{where } P_{\tilde{\beta}}A_{\tilde{\beta}} + A_{\tilde{\beta}}^\top P_{\tilde{\beta}} = -I_2. \tag{11}$$

Since $A_{\tilde{\beta}}$ is Hurwitz, a symmetric positive definite $P_{\tilde{\beta}}$ as defined above exists, and

$$\lambda_{\min}(P_{\tilde{\beta}})\left\|\tilde{\boldsymbol{\beta}}\right\|^2 \le V_{\tilde{\beta}} \le \lambda_{\max}(P_{\tilde{\beta}})\left\|\tilde{\boldsymbol{\beta}}\right\|^2,\quad \dot{V}_{\tilde{\beta}} = -\left\|\tilde{\boldsymbol{\beta}}\right\|^2.$$

Define the positively invariant set $\Omega_{\tilde{\beta}} = \{V_{\tilde{\beta}} \le c_{\tilde{\beta}}\}$. Choosing the positive constant $c_{\tilde{\beta}} = \lambda_{\min}(P_{\tilde{\beta}})\delta^2$ implies that $\left\|\tilde{\boldsymbol{\beta}}(t)\right\| \le \delta$ and hence $|\tilde{\beta}_1(t)| < \delta$ as required.

A Lyapunov function for the platform tracking error can be taken as

$$V_{\boldsymbol{e}} = \boldsymbol{e}^\top P_{\boldsymbol{e}}\boldsymbol{e}, \quad \text{where } P_{\boldsymbol{e}}A_{\boldsymbol{e}} + A_{\boldsymbol{e}}^\top P_{\boldsymbol{e}} = -I_6. \tag{12}$$

Taking the derivative of (12) and considering the potential for tracking error in $\boldsymbol{\beta}$ yields

$$\begin{aligned}
\dot{V}_{\boldsymbol{e}} &= -\left\|\boldsymbol{e}\right\|^2 + 2[0_{3\times 1}^\top, \boldsymbol{e}_\beta^\top]P_{\boldsymbol{e}}\boldsymbol{e},\\
&\le -\left\|\boldsymbol{e}\right\|^2 + 2\lambda_{\max}(P_{\boldsymbol{e}})\left\|\boldsymbol{e}_\beta\right\|\left\|\boldsymbol{e}\right\|.
\end{aligned} \tag{13}$$

Since $\boldsymbol{e}_\beta(t, \boldsymbol{q}_1, \tilde{\beta}_1)$ and its partial derivatives are continuous on $\Omega_{\tilde{\beta}}$, and $\boldsymbol{e}_\beta$ is uniformly bounded in time, $\boldsymbol{e}_\beta$ is locally Lipschitz in $\tilde{\beta}_1$ on $\Omega_{\tilde{\beta}}$. Hence, in $\Omega_{\tilde{\beta}}$

$$\left\|\boldsymbol{e}_\beta(t, \boldsymbol{q}_1, \tilde{\beta}_1) - \boldsymbol{e}_\beta(t, \boldsymbol{q}_1, 0)\right\| \le L\left\|\tilde{\beta}_1\right\| \le L\delta. \tag{14}$$

This enables us to bound the Lyapunov derivative (13) by

$$\dot{V}_{\boldsymbol{e}} \leq -\left\|\boldsymbol{e}\right\|^2 + 2\lambda_{\max}(P_{\boldsymbol{e}})L\delta\left\|\boldsymbol{e}\right\|. \tag{15}$$

Therefore, for $\left\|\boldsymbol{e}\right\| > 2\lambda_{\max}(P_{\boldsymbol{e}})L\delta$, $\dot{V}_{\boldsymbol{e}} < 0$. Using the bounds $\lambda_{\min}(P_{\boldsymbol{e}})\left\|\boldsymbol{e}\right\|^2 \leq V_{\boldsymbol{e}} \leq \lambda_{\max}(P_{\boldsymbol{e}})\left\|\boldsymbol{e}\right\|^2$, we can ensure $\Omega_{\boldsymbol{e}} = \{V_{\boldsymbol{e}} \leq c_{\boldsymbol{e}}\}$ is a positively invariant set with the following choice of $c_{\boldsymbol{e}}$

$$c_{\boldsymbol{e}} \geq \lambda_{\max}(P_{\boldsymbol{e}})(2\lambda_{\max}(P_{\boldsymbol{e}})L\delta)^2. \tag{16}$$

This leads to the domain of operation $\Omega = \Omega_{\tilde{\beta}} \times \Omega_{\boldsymbol{e}}$ which is compact and positively invariant under state feedback.

B. Stability under State Feedback

Lemma 1 (Stability under State Feedback): For the closed-loop system under state feedback (7), with initial tracking error $(\boldsymbol{e}(0), \tilde{\boldsymbol{\beta}}(0)) \in \Omega$, the system states $(\boldsymbol{e}(t), \tilde{\boldsymbol{\beta}}(t))$ remain in Ω for all $t > 0$ and exponentially converge to the origin.

Proof: The closed-loop system (7) is a cascade system of the form

$$\begin{aligned}
\dot{\boldsymbol{e}}_1 &= \boldsymbol{e}_2,\\
\dot{\boldsymbol{e}}_2 &= -k_1\boldsymbol{e}_1 - k_2\boldsymbol{e}_2 + \boldsymbol{e}_\beta(t, \boldsymbol{q}_1, \tilde{\beta}_1),\\
\dot{\tilde{\beta}}_1 &= \tilde{\beta}_2,\\
\dot{\tilde{\beta}}_2 &= -k_3\tilde{\beta}_1 - k_4\tilde{\beta}_2.
\end{aligned}$$

The Lyapunov functions for the platform tracking error (12) and the carrier UAV rotational tracking error (11) can be combined to form a composite Lyapunov function

$$V = dV_e + V_{\tilde{\beta}}, \quad d > 0. \tag{17}$$

Following the generalized proof for cascaded system stability in [26], the closed-loop state feedback system converges exponentially to the origin and Ω is compact and positively invariant for d chosen small enough. ■

C. Stability under Output Feedback

The system under output feedback is a singularly perturbed system which can be separated into two time-scales. The system dynamics and control reside in the slow time-scale while the observer resides in the fast time-scale.

Lemma 2 (Convergence of EHGO Estimates): The estimates, $\hat{\boldsymbol{\chi}}$, converge to an $O(\epsilon)$ neighborhood of the true state, $\boldsymbol{\chi}$, for any $\epsilon \in (0, \epsilon^*)$ for sufficiently small $\epsilon^* > 0$.
The lemma follows from standard high-gain observer analysis [27].

Remark 1: It follows from standard EHGO analysis that the estimation error enters an invariant set contained inside a ball of radius ϵc after some short time $T(\epsilon)$, where $\lim_{\epsilon\to 0} T(\epsilon) = 0$ and $c \in \mathbb{R}_{>0}$. Since the initial state resides on the interior of Ω, choosing ϵ sufficiently small ensures that the states will not leave Ω during the interval $[0, T(\epsilon)]$, thus the system state will remain inside the domain of operation under output feedback while the observer converges.

Theorem 1 (Stability under Output Feedback): The closed-loop tracking error system under output feedback, with initial conditions on the interior of Ω, exponentially converges to an $O(\epsilon)$ neighborhood of the origin when ϵ is chosen small enough.

Proof: The output feedback closed-loop system can be written in singularly perturbed form. The system dynamics form the reduced system and the observer dynamics form the boundary layer system. This system has a two time-scale structure as ϵ becomes small. The boundary layer system has an exponentially stable equilibrium point at the origin from Lemma 2. The reduced system also has an exponentially stable equilibrium point at the origin as shown in Lemma 1. Following Theorem 11.4 in [28], it can be shown that the entire closed-loop output feedback system is exponentially stable when ϵ is chosen sufficiently small. ■

V. Simulation

The estimation and control strategy presented above is simulated to perform trajectory tracking in the flat outputs, $\boldsymbol{q}_1$, i.e, platform pose. A simple task is chosen where the platform is taken from an initial position and orientation, $\boldsymbol{q}_1 = [0, 0, 0]^\top$, to a final position and orientation, $\boldsymbol{q}_1 = [1, 1, 1]^\top$. The system then returns back to the initial configuration. As the controller requires continuous derivatives of the desired trajectory, $\boldsymbol{q}^d$, up to fifth order, the desired trajectory $\boldsymbol{q}^d(t)$ is taken as a 9-th order polynomial with given initial and final values: $\boldsymbol{q}^d(t=0) = [0, 0, 0]^\top$, and $\boldsymbol{q}^d(t=5) = [1, 1, 1]^\top$. The derivatives up to 5-th order are set to zero at $t = 0$ and $t = 5$. The return trajectory is generated in the same manner, but in the opposite direction. The simulation is conducted with the disturbances $\boldsymbol{\sigma}_q = [\sin(2t), \sin(3t), \sin(t)]^\top$ and $\sigma_\beta = \sin(4t)$ applied to the system dynamics. Plots of the desired and actual trajectories under output feedback control are shown in Fig. 2.

VI. Conclusions

We studied a novel long reach aerial manipulation system in which a small horizontally actuated platform is suspended from a larger carrier UAV. Modeling error and external disturbances are considered in the control design. An EHGO is designed to estimate unmeasured states and system uncertainties which can be canceled through a feedback linearizing control design. The method is shown to be effective in simulation and is proven to be stable.

We plan to extend this work in a number of directions. We will conduct experiments to show the viability of the control design on a physical system. Furthermore, we plan to extend the control methodology from the planar case to the full three-dimensional case.

References

[1] G. Garimella and M. Kobilarov, "Towards model-predictive control for aerial pick-and-place," in *International Conference on Robotics and Automation (ICRA)*, pp. 4692–4697, IEEE, 2015.

[2] J. Thomas, J. Polin, K. Sreenath, and V. Kumar, "Avian-inspired grasping for quadrotor micro UAVs," in *International Design Engineering Technical Conferences and Computers and Information in Engineering Conference*, ASME, 2013.

[3] J. Thomas, G. Loianno, K. Sreenath, and V. Kumar, "Toward image based visual servoing for aerial grasping and perching," in *International Conference on Robotics and Automation (ICRA)*, pp. 2113–2118, IEEE, 2014.

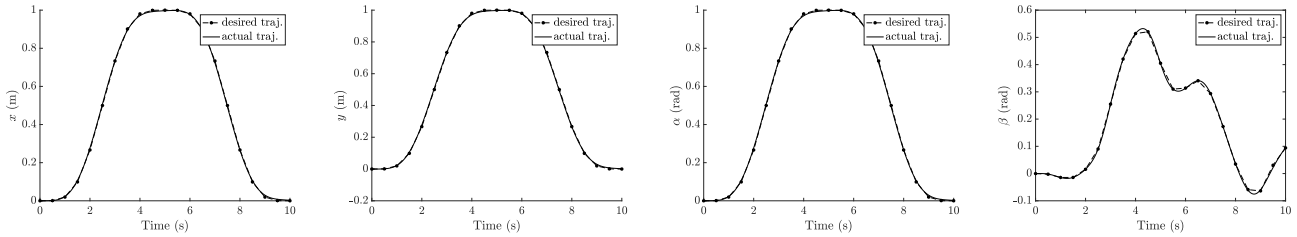

(a) Desired and actual trajectories: x (b) Desired and actual trajectories: y (c) Desired and actual trajectories: α (d) Desired and actual trajectories: β

Fig. 2. Trajectory tracking for x, y, α (platform pose) and β (UAV orientation) under output feedback control in the presence of disturbances.

[4] M. Orsag, C. Korpela, and P. Oh, "Modeling and control of MM-UAV: Mobile manipulating unmanned aerial vehicle," *Journal of Intelligent & Robotic Systems*, vol. 69, no. 1-4, pp. 227–240, 2013.

[5] S. Kim, S. Choi, and H. J. Kim, "Aerial manipulation using a quadrotor with a two DOF robotic arm," in *International Conference on Intelligent Robots and Systems*, pp. 4990–4995, IEEE, 2013.

[6] G. Heredia, A. Jimenez-Cano, I. Sanchez, D. Llorente, V. Vega, J. Braga, J. Acosta, and A. Ollero, "Control of a multirotor outdoor aerial manipulator," in *International Conference on Intelligent Robots and Systems (IROS)*, pp. 3417–3422, IEEE, 2014.

[7] A. Jimenez-Cano, J. Martin, G. Heredia, A. Ollero, and R. Cano, "Control of an aerial robot with multi-link arm for assembly tasks," in *International Conference on Robotics and Automation (ICRA)*, pp. 4916–4921, IEEE, 2013.

[8] C. Korpela, M. Orsag, and P. Oh, "Towards valve turning using a dual-arm aerial manipulator," in *International Conference on Intelligent Robots and Systems (IROS)*, pp. 3411–3416, IEEE, 2014.

[9] D. Orol, J. Das, L. Vacek, I. Orr, M. Paret, C. J. Taylor, and V. Kumar, "An aerial phytobiopsy system: Design, evaluation, and lessons learned," in *International Conference on Unmanned Aircraft Systems (ICUAS)*, pp. 188–195, IEEE, 2017.

[10] K. Sreenath, T. Lee, and V. Kumar, "Geometric control and differential flatness of a quadrotor UAV with a cable-suspended load," in *Conference on Decision and Control (CDC)*, pp. 2269–2274, IEEE, 2013.

[11] P. J. Cruz and R. Fierro, "Cable-suspended load lifting by a quadrotor UAV: hybrid model, trajectory generation, and control," *Autonomous Robots*, vol. 41, no. 8, pp. 1629–1643, 2017.

[12] P. O. Pereira, M. Herzog, and D. V. Dimarogonas, "Slung load transportation with a single aerial vehicle and disturbance removal," in *Mediterranean Conference on Control and Automation (MED)*, pp. 671–676, IEEE, 2016.

[13] N. Michael, J. Fink, and V. Kumar, "Cooperative manipulation and transportation with aerial robots," *Autonomous Robots*, vol. 30, no. 1, pp. 73–86, 2011.

[14] T. Lee, "Geometric control of quadrotor UAVs transporting a cable-suspended rigid body," *IEEE Transactions on Control Systems Technology*, vol. 26, no. 1, pp. 255–264, 2017.

[15] P. O. Pereira and D. V. Dimarogonas, "Nonlinear pose tracking controller for bar tethered to two aerial vehicles with bounded linear and angular accelerations," in *Conference on Decision and Control (CDC)*, pp. 4260–4265, IEEE, 2017.

[16] D. Sanalitro, H. J. Savino, M. Tognon, J. Cortés, and A. Franchi, "Full-pose manipulation control of a cable-suspended load with multiple UAVs under uncertainties," *IEEE Robotics and Automation Letters*, 2020.

[17] P. O. Pereira and D. V. Dimarogonas, "Pose and position trajectory tracking for aerial transportation of a rod-like object," *Automatica*, vol. 109, p. 108547, 2019.

[18] H.-N. Nguyen, S. Park, J. Park, and D. Lee, "A novel robotic platform for aerial manipulation using quadrotors as rotating thrust generators," *IEEE Transactions on Robotics*, vol. 34, no. 2, pp. 353–369, 2018.

[19] A. Suarez, A. Giordano, K. Kondak, G. Heredia, and A. Ollero, "Flexible link long reach manipulator with lightweight dual arm: Soft-collision detection, reaction, and obstacle localization," in *International Conference on Soft Robotics (RoboSoft)*, pp. 406–411, IEEE, 2018.

[20] M. J. Kim, J. Lin, K. Kondak, D. Lee, and C. Ott, "Oscillation damping control of pendulum-like manipulation platform using moving masses," *IFAC-PapersOnLine*, vol. 51, no. 22, pp. 465–470, 2018.

[21] A. Suárez, P. Sanchez-Cuevas, M. Fernandez, M. Perez, G. Heredia, and A. Ollero, "Lightweight and compliant long reach aerial manipulator for inspection operations," in *International Conference on Intelligent Robots and Systems (IROS)*, pp. 6746–6752, IEEE, 2018.

[22] Y. S. Sarkisov, M. J. Kim, D. Bicego, D. Tsetserukou, C. Ott, A. Franchi, and K. Kondak, "Development of SAM: Cable-suspended aerial manipulator," in *International Conference on Robotics and Automation (ICRA)*, pp. 5323–5329, IEEE, 2019.

[23] R. Miyazaki, H. Paul, T. Kominami, and K. Shimonomura, "Wire-suspended device control based on wireless communication with multirotor for long reach-aerial manipulation," *IEEE Access*, vol. 8, pp. 172096–172104, 2020.

[24] A. Suarez, F. Real, V. M. Vega, G. Heredia, A. Rodriguez-Castaño, and A. Ollero, "Compliant bimanual aerial manipulation: Standard and long reach configurations," *IEEE Access*, vol. 8, pp. 88844–88865, 2020.

[25] C. J. Boss, J. Lee, and J. Choi, "Uncertainty and disturbance estimation for quadrotor control using extended high-gain observers: Experimental implementation," in *Dynamic Systems and Control Conference (DSCC)*, vol. 58288, p. V002T01A003, ASME, 2017.

[26] C. J. Boss, V. Srivastava, and H. K. Khalil, "Robust tracking of an unknown trajectory with a multi-rotor UAV: A high-gain observer approach," in *American Control Conference*, (Denver, CO), pp. 1429–1434, July 2020. Extended version available at: arXiv preprint arXiv:2003.06390.

[27] H. K. Khalil, *High-Gain Observers in Nonlinear Feedback Control*. Society for Industrial and Applied Mathematics, 2017.

[28] H. K. Khalil, *Nonlinear Systems*. Prentice Hall, third ed., 2002.